Biomineralization of PbS and PbS–CdS core–shell nanocrystals and their application in quantum dot sensitized solar cells†

Leah C. Spangler,[a] Li Lu,[b] Christopher J. Kiely,[ab] Bryan W. Berger*[ac] and Steven McIntosh*[a]

Biomineralization utilizes biological systems to synthesize functional inorganic materials for application in diverse fields. In the current work, we enable biomineralization of quantum confined PbS and PbS–CdS core–shell nanocrystals and demonstrate their application in quantum dot sensitized solar cells (QDSSCs). An engineered strain of Stenotrophomonas maltophilia is utilized to generate a cystathionine g-lyase that is active for the biomineralization of metal sulfide nanocrystals from a buffered aqueous solution of metal salts and L-cysteine. In the presence of lead acetate, this enzymatic route generates rock salt structured PbS nanocrystals. Controlling the growth conditions yields 4 nm PbS crystals with absorption and photoluminescence peaks at 910 nm and 1080 nm, respectively, consistent with the expected strong quantum confinement of PbS at this size. Quantum yields (QY) of the biomineralized PbS quantum dots, determined after phase transfer to the organic phase, range between 16 and 45%. These are the highest reported QY values for any biomineralized quantum dot materials to date and are comparable with QYs reported for chemically synthesized materials. Subsequent exposure to cadmium acetate results in the biomineralization of a thin CdS shell on the PbS core with a resultant blue-shift in optical properties. The photoluminescence peak shifts to 980 nm, consistent with the expected decrease in band gap energy of a PbS–CdS core–shell heterostructured quantum dot. HAADF-STEM imaging confirms the crystalline structure and size of the particles with complimentary XEDS analysis confirming the presence of Cd, Pb, and S in individual nanocrystals. Integration of these QDs into QDSSCs yields open circuit potentials of 0.43 V and 0.59 V for PbS and PbS–CdS, respectively, consistent with expectations for these materials and previously reported values for chemically synthesized QDs.

Introduction

Biomineralization is the process whereby biological systems and molecules catalyze and direct the formation of inorganic materials.[1,2] In contrast to typical chemical synthesis schemes, biomineralization and bio-inspired synthesis approaches promise aqueous phase green synthesis of inorganic materials at physiological temperatures. The most commonly studied systems are those found in nature for the formation of structural materials, such as $CaCO_3$ (ref. 3–5) and SiO_2.[6–9] While great advances have been made in our understanding of these systems, the focus needs to shi from structural to functional materials in order for biomineralization to have an impact on energy applications. A recent demonstration of the potential of this approach is the application of a-Fe_2O_3 (prepared by bio-mineralization using Acidovorax sp.) as an electrode material for Li-ion batteries.[10] In addition to the greening of the material synthesis process, the textural enhancement in a-Fe_2O_3 ach-ieved through biomineralization was shown to improve battery capacity and charge retention upon cycling at high rate.

In the current work, we describe a new and facile approach to biomineralization of quantum con ned PbS and PbS–CdS core– shell nanocrystals from aqueous solutions of precursor metal salts using the amino acid L-cysteine as a sulfur source and capping agent. An engineered strain of Stenotrophomonas mal-tophilia was utilized to generate a putative g-cystathionine lyase that catalyzes nanocrystal biomineralization by the in situ enzymatic generation of reactive sulfur from the amino acid L-cysteine.[11] Switching the metal precursor in the growth medium from a Pb salt to a Cd salt enables CdS shell biomineralization on a PbS core which gives rise to the expected blue-shi in optical properties relative to pure PbS QD's. To the best of our

[a]Department of Chemical and Biomolecular Engineering, Lehigh University, Bethlehem, PA 18015, USA. E-mail: mcintosh@lehigh.edu; berger@lehigh.edu

[b]Department of Materials Science and Engineering, Lehigh University, Bethlehem, PA 18015, USA

[c]Program in Bioengineering, Lehigh University, Bethlehem, PA 18015, USA

† Electronic supplementary information (ESI) available. See DOI: 10.1039/c5ta10534j

knowledge, this is the rst report of biomineralized core–shell quantum dot nanocrystal morphology formed without the addition of a reactive chemical precursor such as Na_2S. The potential of this synthesis approach to impact energy applica-tions is demonstrated by incorporating the biomineralized PbS and PbS–CdS nanomaterials into quantum dot sensitized solar cells.

Previously, we demonstrated the ability of S. maltophilia to synthesize size controlled CdS nanocrystals.[11] The current work illustrates the generality of our method by showing that the same strain of S. maltophilia can be used to produce PbS nanocrystals without any further evolution. In addition, we are able to synthesize PbS–CdS core–shell structures using this low temperature biosynthetic route without having to resort to using a conventional chemical route to deposit the shell material.

PbS nanocrystal quantum dots have a relatively large Bohr radius (18–20 nm)[12] with an easily accessible quantum con nement region, which makes them highly interesting for energy harvesting applications. The strong quantum con ne-ment eff ects displayed by sub-20 nm PbS particles leads to highly tunable band-gap energies that can be several times greater than that of the bulk PbS material (0.41 eV). This tunable band gap, when coupled with the smaller intrinsic line width exhibited by nanocrystals signi cantly below the Bohr radius, can lead to enhancements in non-linear optical properties.[12,13] Such PbS nanocrystals are an ideal candidate for use in quantum dot sensitized solar cells as they can be designed to absorb in the near infrared, optimally harvesting light in the peak region of the solar spectral range.[14] Additionally, PbS quantum dots are potential multi-exciton generators[15,16] which can be used to further improve solar cell efficiency by breaking the Shockley–Queisser limit.[17] Core–shell morphology PbS–CdS nanocrystals are also of interest due to the further enhancement of the non-linear optical properties they off er when compared with the basic PbS core materials. For example, Neo et al. demonstrated a signi cant increase in free-carrier absorption upon growth of a CdS shell on PbS QD cores in materials prepared by conventional methods.[18] Within a quantum dot sensitized solar cell environment the PbS–CdS core–shell morphology was found to lead to an increased electron lifetime, a decreased electron transit time and an increased photo-stability through passivation of PbS surface defects.[19]

As noted recently by Hens,[20] a signi cant practical issue that hinders the application of these PbS-based quantum dot materials in solar cell technologies is the simple fact that the typical hot-injection synthesis method is expensive and there-fore incompatible with the low-cost requirements of the solar cell device. The biomineralization approach described herein demonstrates that a low cost, room temperature, aqueous phase synthesis of crystalline quantum con ned PbS and PbS–CdS core–shell quantum dots is now possible.

Previous reports of metal sul de biomineralization can be broadly grouped into two distinct categories. Either (i) sulfur-containing molecules that are naturally abundant within an organism are utilized for mineralization as a response to the presence of a heavy metal, or (ii) a biomolecule is utilized to template nanoparticle mineralization in the presence of an added reactive chemical precursor such as Na_2S. In the latter approach, the Na_2S will react with the metal salt to form metal sul des in solution; the biomolecule is required to template and direct the formation of nanocrystals rather than generating 'bulk' crystalline materials.

Reports describing PbS biomineralization utilizing the rela-tively low levels of metabolic sulfur naturally present in an organism have been published previously by a number of groups.[21–24] However, these studies report optical properties for the resultant nanoparticulate material that are inconsistent with the known size-dependence of the PbS band gap energy, which casts doubt on the actual identity of the nal product.[21–24] Furthermore, the mineralization process is either intracellular, requiring cell lysis and puri cation to harvest the nano-crystals,[21,22] or anaerobic,[23] which limits the scale and throughput of production, or occurs over very long time periods (>24 h).[24] Furthermore, the use of only endogenous levels of sulfur required for basic cellular processes most likely limits the total yield of nanomaterial. An alternative bio-templating approach demonstrated by Ma et al.[25] utilized a luciferase enzyme to template 5 nm PbS quantum dots upon addition of Na_2S to a Pb-containing precursor solution. Unlike the prior purely biological approaches, this hybrid biological–chemical approach did yield materials whose optical characteristics were consistent with the established optical properties of PbS nano-crystals. All these previous approaches for PbS biomineralization are distinctly diff erent from the approach reported herein. We present the rst purely biological approach to extracellular PbS quantum dot biomineralization via the enzymatic turnover of an abundant bioprecursor, L-cysteine, when added to a solution of lead acetate and an engineered strain of S. maltophilia. Furthermore, the system is shown to be unreactive in the absence of any one of these three critical components.

The potential for functional PbS-based nanomaterials prepared by biomineralization to have an impact in the energy harvesting arena is further demonstrated in our current work by the subsequent biomineralization of a CdS shell onto the PbS QD core. When integrated into a quantum dot sensitized solar cell our biomineralized PbS–CdS core–shell nanocrystals provide the expected increase in open circuit potential when compared to PbS QD sensitized solar cells.[26] To the best of our knowledge, the only prior reports of biosynthesis of semi-conductor core–shell particles utilize a hybrid biological– chemical approach for templating a chemical reaction with a biomolecule. Singh et al. utilized an engineered peptide to form CdSe QDs from the reactive chemical precursor NaHSe, and then grew a ZnS shell on the CdS seed using the reactive chemical precursor Na_2S.[27] Kong et al. utilized the reactive chemical precursor Na_2SeSO_3 in bovine serum albumin to generate larger Ag_2Se–Se core–shell nanoparticles.[28] In both of these studies, one or more reactive chemical precursors had to be combined with templating biomolecules for nanomaterial synthesis to occur, whereas in our approach both templating and reactive chemical precursor formation are achieved in a single, cellular process using non-reactive lead acetate and L-cysteine precursors.

Experimental

Biomineralization of CdS quantum dot nanocrystals by a strain of Stenotrophomonas maltophilia (SMCD1) has previously been demonstrated.[11] This strain was engineered for Cd tolerance from a wild-type by directed evolution and this same strain is utilized in the current study without any further engineering.

SMCD1 was sub-cultured into 100 mL of lysogeny broth and grown for 12 h at 37 C with shaking. Cells were collected by centrifugation at 5000 rpm for 10 minutes and re-suspended in aqueous Tris–HCl buffer (0.1 M, pH 7.5). For particle growth, an aqueous solution of lead acetate (1 mM, Alfa Aesar Puratronic, 99.995% metals basis), L-cysteine (8 mM, Spectrum Chemicals, 99.55%) and Tris–HCl buffer (pH 7.5) was chilled on ice prior to addition of re-suspended SMCD1 cells (OD_{600} ¼ 0.5). The solution was kept on ice during growth. Following incubation for 5 min, the cells were removed by centrifuging the solution at 8000 rpm for a further 5 min. The supernatant was then collected and kept at 18 C for a series of prescribed time periods. Note that PbS growth continues during this incubation phase due to the presence of a g-cystathionine lyase enzyme produced by SMCD1 in response to heavy metal toxicity stress. This enzyme has previously been demonstrated to be impli-cated in the biomineralization of CdS using SMCD1.[11] We con rmed this same enzyme is also associated with PbS nano-crystal biomineralization using the same procedure, in which a synthesized batch of nanocrystals was dialyzed against DI water for 24 hours, lyophilized and the proteins associated with puri ed PbS nanocrystals directly identi ed from dried samples via electrospray ionization mass spectrometry (Fig. S1†).

For CdS shell growth, as grown PbS QDs in the aqueous phase were further concentrated using centrifugation at 12 000 rpm for 10 minutes. The supernatant was discarded and the particles re-suspended in an aqueous solution of L-cysteine (8 mM). Cadmium acetate (1 mM, Alfa-Aesar Puratronic, 99.999% metals basis) and tetramethylammonium hydroxide (5 mM, Alfa Aesar, 98%) were added and the solution was incubated at 37 C for 18 h.

Phase transfer of the as-prepared PbS or PbS–CdS QDs from aqueous to organic solvents was performed following the procedure developed by Gaponik et al.[29] 5 mL of aqueous QD solution was placed in a glass vial, followed by addition of 5 mL 1-dodecanethiol (DDT) and then 5 mL acetone. The mixture was then vigorously agitated for 15 min at 60 C. A er phase transfer, the organic phase was withdrawn and mixed with an equal volume of toluene. Finally, the DDT capped nanocrystals were precipitated with methanol and then re-suspended in chloroform or tetrachloroethylene for subsequent optical absorption and uorescence measurements.

Optical absorbance measurements were performed using a Shimadzu UV-vis 2600 spectrophotometer equipped with an ISR-2600-Plus integrating sphere attachment. Photo-luminescence spectra were acquired using a Horiba Fluorolog-3 equipped with a liquid nitrogen cooled InGaAs detector. To inhibit further nanocrystal growth during aqueous photo-luminescence measurements, each sample was chilled on ice for 2 min and the temperature controller was set to 5 C. Quantum yields, QYs, were determined using the reference dye IR-26 in 1,2-dichloroethane.[30] Powder XRD measurements were performed on precipitated, dried QDs using Cu K_a (1.5418 A) radiation in a Rigaku Mini ex II diffractometer. Samples suit-able for electron microscopy analysis were obtained by drop-casting puri ed and diluted PbS or PbS–CdS organic phase solutions onto a holey carbon coated grid and allowing the solvent to evaporate. The samples were analyzed at 200 kV in an aberration corrected JEOL ARM 200CF analytical electron microscope equipped with a JEOL Centurio XEDS system.

Solar cell structures were fabricated on uorine doped tin oxide (FTO) coated glass slides (Sigma Aldrich, 7 U sq ^{1}) that were cleaned by a three stage process. Firstly, by sonication in a 50 : 50 ethanol- to acetone mixture, secondly, by sonication in a 1 : 10 Contrad 70 soap to DI water solution, and nally, by sonication in 200 proof ethanol. The cleaned FTO substrates were then rinsed with 200 proof ethanol and blown dry with N_2. A TiO_2 blocking layer was then deposited using a modi ed convective deposition method described below.[31] The cleaned FTO substrate was held horizontally and placed in contact with an inclined glass microscope slide touching at a 45 angle. The lower side of the inclined glass slide was rendered hydrophobic using para lm. Next, 15 mL of a titanium(IV)butoxide precursor solution was placed in the wedge formed between the FTO and glass slide, and the substrate was pushed using a linear motor in order to spread the solution uniformly across the FTO slide. A er deposition, the material was annealed at 500 C for 3 hours to form the TiO_2 blocking layer. Following this, a macro-porous TiO_2 layer was deposited onto a 1 cm^2 area of the FTO with TiO_2 blocking layer using an opaque titania paste (Sigma Aldrich) applied with the doctor blade method and then annealed at 500 C for 1.5 h. The PbS or PbS–CdS quantum dots were deposited onto the TiO_2 electrode by a sequence of 20 drop-casting/drying steps of the organic colloidal solutions. A gold anode was deposited by the doctor blade technique on a cleaned FTO surface and annealed at 200 C for 1 h. The solar cell structures were completed by sandwiching 15 mL of 0.5 M polysul de electrolyte[32] between the TiO_2-quantum dot substrate and the anode using a para lm spacer. The current density–voltage (J–V) characteristics of the solar cell were measured using a Gamry instruments electrochemical work-station operating under AM 1.5 (100 mW cm^{2}) illumination conditions created by an ABET Technologies (Model no. 10500) solar simulator.

Results and discussion

Strain SMCD1 was originally evolved to produce CdS nano-crystals from aqueous solutions of Cd acetate, L-cysteine in M9 minimal media at 37 C.[11] Replacing cadmium acetate in this preparation with lead acetate under the same concentration and temperature conditions leads to formation of an opaque brown solution within 20 minutes. XRD analysis of centrifuged and dried solid a er 3 hours of growth, Fig. 1a, shows a diffraction pattern consistent with the cubic rock salt phase of PbS (JCPDS #5-592). This precipitate is only formed in

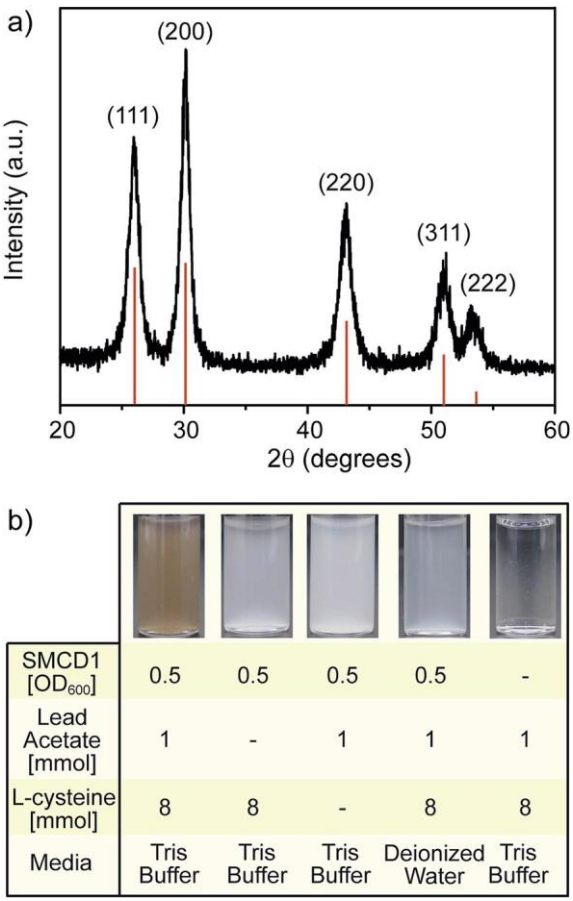

Fig. 1 (a) X-ray diffraction pattern obtained from the brown precipi-tate formed after 3 hours at 37 C in a Tris buffered (pH 7.5) aqueous solution of lead acetate, L-cysteine, and strain SMCD1. (b) Matrix of reaction ingredients and the corresponding photographs of solutions containing all components and those with one component deliber-ately missing.

a buffered aqueous solution in the presence of strain SMCD1, lead acetate, and L-cysteine. Removal of any of these compo-nents, including utilizing unbuffered de-ionized water, does not lead to the formation of a brown precipitate. The solutions without all components present appear turbid due to the optical density of the cell suspension (Fig. 1b). The solution that does not contain L-cysteine is more opaque due to the formation of a white precipitate, most likely $Pb(OH)_2$, which forms due to the absence of L-cysteine as the metal complexing agent. Note that the cells were not centrifuged from any of these samples shown in Fig. 1b during PbS growth.

The ability of the same strain of S. maltophilia to indepen-dently produce both CdS and PbS nanocrystals clearly demon-strates its exibility in synthesizing various metal sul de quantum dots. SMCD1 is therefore facilitating biomineraliza-tion of PbS from solution in an analogous manner to that described in our previous reports of CdS biomineralization. This observation is consistent with the known heavy metal tolerance of S. maltophilia.[33]

The driving mechanism underlying this mineralization process is most likely through the expression of a putative cystathionine g-lyase (smCSE) previously found to be associated with the extracellular biomineralization of CdS quantum dot nanocrystals from SMCD1.[11] Cystathionine g-lyases are a class of enzymes that catalyze the production of H_2S, NH_3 and pyruvate from L-cysteine; we propose that the reactive H_2S thus generated leads to the mineralization of PbS. This concept of enzymatic generation of reactive sulfur has been suggested in a number of prior studies focused on CdS biomineralization, typically utilizing endogenous levels of sulfur-containing biomolecules present in the cells.[34–38] In the present case, the addition of excess L-cysteine beyond endogenous levels provides both an abundant sulfur source and a useful nanoparticle capping agent.[39–44]

The calculated crystallite size by the Scherrer equation for the data in Fig. 1 is 7 nm. Modi cation of the synthesis proce-dure was necessary in order to access the strong quantum con ned size range with optical properties in the desirable near-IR range.[45] Building on the hypothesis that bio-mineralization occurs via a cystathionine g-lyase catalyzed H_2S generation from L-cysteine, and noting prior literature demon-strating that a decreased supply rate of H_2S results in a decrease in average PbS crystallite size during chemical synthesis,[46] the biomineralization rate was deliberately lowered by reducing the rate of H_2S generation. To achieve this goal, the solution was placed on ice during initial nanocrystal nucleation and the SMCD1 cells centrifuged from solution a er 5 min of growth time. The aqueous centrifuged supernatant was buffered at pH 7.5 and contained residual lead acetate, L-cysteine and enzyme produced by the cells during the rst 5 min of growth; removal of the cells was implemented to halt production of additional enzyme and thus limit growth rate. The temperature for subsequent nanocrystal growth in the centrifuge supernatant was carefully controlled at 18 C for a variety of time periods. The presence of the expected cystathionine g-lyase associated with the PbS nanocrystals was indeed con rmed by electrospray ionization mass spectrometry (Fig. S1†).

Fig. 2 shows a systematic series of photoluminescence spectra obtained from the aqueous solution at various incuba-tion time intervals between 15 and 95 minutes following centrifugation and removal of the cells. The apparent photo-luminescence peak is seen to red-shi with increasing incuba-tion time from 1040 nm a er 15 min to 1135 nm a er 95 min. It should be noted, however, that the true maximum of the uo-rescence peak is obscured due to the overlapping absorption pro le of water in this region, as indicated by the dotted line in Fig. 2. This unfortunate overlap combined with the low concentration of PbS nanocrystals present inhibited our ability to collect the corresponding absorption spectral data as a func-tion of incubation time. The peak luminescence positions and red-shi with increasing incubation time are however entirely consistent with those expected for a gradual increase in the average size of quantum con ned PbS nanocrystals with increasing growth time.[12,47,48] The bulk direct band gap for PbS is 0.41 eV (3024 nm) and the excitonic Bohr radius is 18 nm, and reports suggest that strong quantum con nement effects should occur for particles below 8 nm in diameter.[47] While we cannot determine the absorption positions to obtain the direct

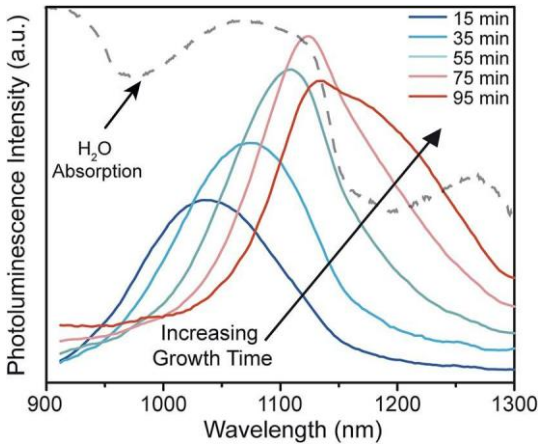

Fig. 2 Photoluminescence spectra obtained from the aqueous PbS nanocrystal solution as a function of incubation time at 18 C. The observed red-shift of the peak maxima with increasing incubation time is consistent with a gradual increase in average nanocrystallite size within the quantum confined range. The dotted line indicates the expected absorption profile for water.

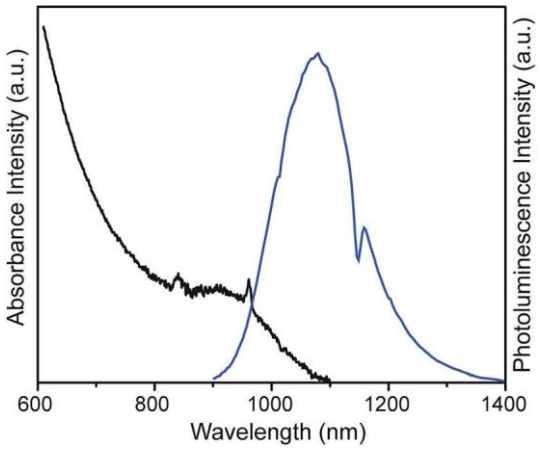

Fig. 3 Absorbance and corresponding photoluminescence spectra of biomineralized PbS nanocrystals grown in the aqueous phase for 30 min following ligand and phase transfer into chloroform. The sharp peaks in the absorbance spectrum (black line) at 820 and 980 nm are artefacts from the instrument detector switch and 1-dodecanethiol (DDT) ligands, respectively. The dip in the photoluminescence spec-trum (blue line) at 1150 nm is due to absorbance from chloroform.

bandgap, calculating a band gap and thus nanocrystallite size from the photoluminescence peak wavelengths of 1040 nm (1.2 eV) and 1135 nm (1.1 eV) leads to maximum mean particle diameters of 3.5 and 4.0 nm, respectively.

The required time (<60 min) for our PbS nanoparticle formation is substantially faster than any other report of PbS biomineralization which typically take 24 to 48 hours at physi-ological temperature.[21,23,24] This is because these prior studies relied solely on utilizing the natural abundance of reactive sulfur generated in the cell in response to Pb exposure. In contrast, in our work the engineered bacterial strain SMCD1 expresses a putative cystathionine g-lyase enzyme in response to exposure to the heavy metals present in solution. This cys-tathionine g-lyase enzyme then actively catalyzes H_2S produc-tion from the excess L-cysteine added to the solution, leading to a much more rapid biomineralization response.

In order to measure the absorption spectrum, the PbS nanocrystals grown in the aqueous phase for 30 min were phase transferred into chloroform with 1-dodecanethiol as capping agent using the method described by Gaponik et al.[29] The resulting absorption and photoluminescence spectra, now free of water absorption artefacts, are shown in Fig. 3, and have maxima at 910 nm and 1080 nm, respectively, which are fully consistent with that expected for quantum con ned PbS nanocrystals of 3.0 nm in size.[12,47,48] The measured full-width-at-half-maximum (FWHM) for the photoluminescence peak from our biomineralized PbS nanocrystals is 144 nm. This FWHM value is consistent with previous reports of bio-templated synthesis of PbS QD.[25,49] For example, Levina et al. report a photoluminescence peak with FWHM of 135 nm at 1060 nm, corresponding to 4 nm QDs.[50] In the absence of any size-selective precipitation steps, PbS QD chemical synthesis in the organic phase typically lead to a FWHM of 100 nm.[51,52] As with other QD materials, post-synthesis size selective precipi-tation, which has not been attempted in our case, can signi cantly narrow the particle size distribution and further improve the FWHM for photoluminescence.

The quantum yield (QY) of the PbS nanocrystals transferred to the organic phase and capped with DDT varied with synthesis batch between 16 and 45%. This batch-to-batch variation and the range of quantum yield is in agreement with previous reports for QDs synthesized from chemically reactive precursors through traditional high temperature approaches, where typical reported QY values range from 20% to 80%.[48,51–55] To the best of our knowledge ours is the highest reported QY for any bio-mineralized PbS quantum dots. There are two previous reports of QY values for bio-templated materials that are particularly relevant to the current study. Firstly, Ma et al. reported a QY value of 3.6% when utilizing luciferase to template the chemical reaction between bound Pb^{2+} and Na_2S.[25] Secondly, Levina et al. reported a QY value of 11.5% when using a DNA template and reactive precursors comprising Pb^{2+} and Na_2S.[49]

The formation of quantum con ned PbS nanocrystals by the biomineralization route has been con rmed by STEM high-angle annular dark eld (HAADF) imaging and X-ray energy dispersive spectroscopy (XEDS) of phase transferred materials. Fig. 4 shows representative electron microscopy data collected from nanocrystals grown for 30 minutes; namely the same material for which optical characterization data are presented in Fig. 3. The PbS nanoparticles are crystalline in nature, exhibiting lattice spacings and interplanar angles consistent with the rock salt structure of PbS (Fig. 4a–d and Table S1†). The nanocrystals have a somewhat irregular shape and are typically around 4.0– 4.5 nm in diameter. This is consistent with the PbS particle size deduced from analysis of the optical properties shown in Fig. 3. The XEDS spectrum obtained on a single nanocrystal, Fig. 4e, con rms the presence of both Pb and S atoms in the particles. Both the M and L families of Pb are identi ed due to the overlap of the Pb M_a and S K_a peak energies.

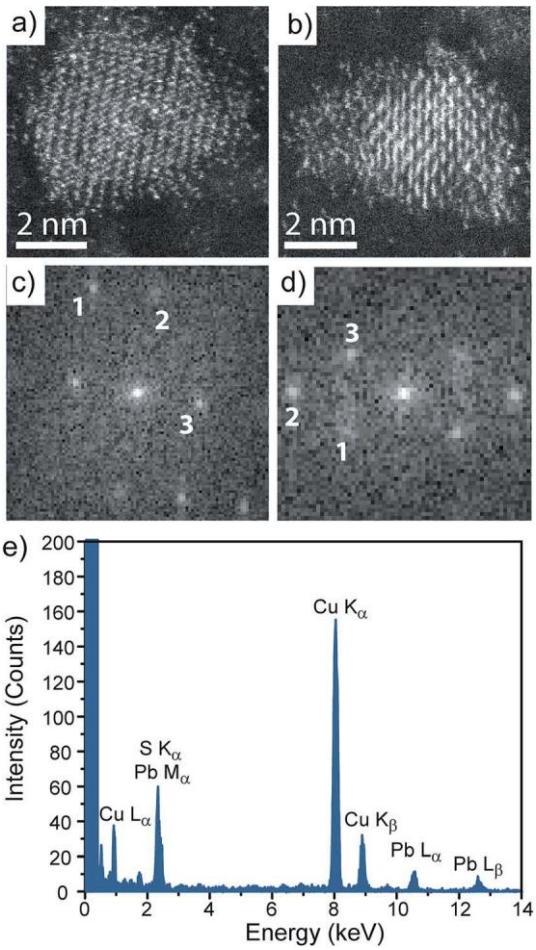

Fig. 4 (a and b) HAADF-STEM images and (c and d) corresponding FFT of 4.5 nm and 4.0 nm PbS nanocrystals viewed along the [112] and [110] projections respectively. Lattice fitting of indicated planes is reported in Table S1.† (e) Representative XEDS spectra acquired from a single biomineralized PbS nanocrystal (30 minutes incubation time at 18 C) showing the co-existence of both Pb and S.

Having established a mechanistic similarity between bio-mineralization of PbS and CdS QDs using S. maltophilia,[11] we attempted to grow a thin CdS shell on the PbS nanocrystal core by a sequential biomineralization process. Speci cally, bio-mineralized PbS cores grown for 30 minutes were concentrated by high speed centrifugation and the supernatant was dis-carded. The PbS nanocrystals were then re-suspended in a pH 7.5 solution of L-cysteine and cadmium acetate. The solution was then incubated at 37 C for 18 hours. The photo-luminescence peak of the resultant PbS–CdS colloidal material shows a progressive blue-shi during this period, which is in good agreement with the expected shi in optical properties induced by the progressive growth of a thin CdS shell on the PbS cores[18,56] (Fig. S2†). No SMCD1 cells were added in this process, instead CdS biomineralization is catalyzed solely by the residual cystathionine g-lyase enzyme associated with the PbS nano-crystals a er centrifugation. No CdS mineralization can occur in the absence of enzyme.[11] Hence, the low concentration of cystathionine g-lyase present in this sequential growth step leads to slow CdS biomineralization ensuring that only a thin CdS shell is formed on the PbS core at the expense of a relatively long growth period.

Fig. 5a shows the photoluminescence spectra of both the original PbS nanocrystals and the PbS–CdS core–shell nano-crystals a er 18 hours of incubation in the cadmium acetate solution and then phase transfer into an organic solvent. The observed blue shi in photoluminescence is characteristic of CdS shell growth on a PbS core,[18,54,57] implying that CdS bio-mineralization has occurred on the PbS nanocrystals. The magnitude of the blue shi is 100 nm, which is indicative of a CdS shell that is 0.4 nm thick,[58] and corresponds to only one or two CdS layers. The corresponding absorbance spectrum for the same PbS–CdS particles is displayed alongside the photo-luminescence spectrum in Fig. 5b. Again, the observed blue-shi in both absorbance and photoluminescence peak posi-tions relative to pure PbS QDs are consistent with the growth of an ultra-thin CdS shell on the PbS core. The measured quantum yield for the PbS–CdS core–shell nanocrystals was 9%. This reduction in QY compared with the parent PbS cores is likely

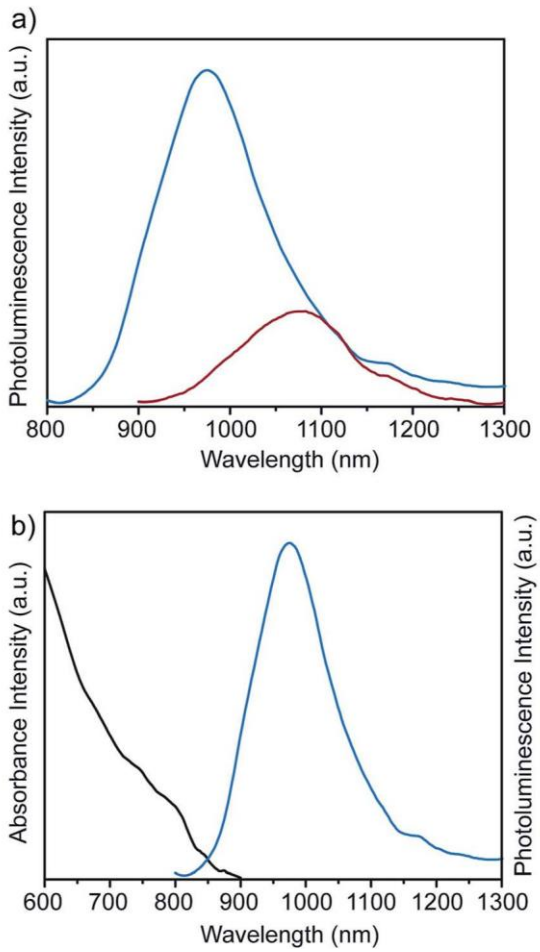

Fig. 5 (a) Photoluminescence spectra of biomineralized PbS (red line) and biomineralized PbS–CdS (blue line) core/shell nanocrystals. (b) Absorbance (black line) and photoluminescence (blue line) spectra of the PbS–CdS core–shell nanocrystals. The above samples were phase transferred into chloroform for optical characterization.

due to the use of DDT capping agent which is well known to quench emission from CdS QDs.[59]

Fig. 6 shows both HAADF-STEM imaging data and XEDS compositional analysis from PbS–CdS morphology nano-crystals. No clearly de ned crystalline CdS shells were detected in the HAADF-STEM images (Fig. 6a and b), which is not entirely unexpected since CdS is not isostructural with the PbS core. Instead, a disordered surface layer about 0.5 nm thick was frequently observed covering the original 3.0–4.0 nm PbS cores. The interior regions of the PbS–CdS particles maintain their original crystalline nature and display lattice spacings and interplanar angles that are fully consistent with the PbS rock salt structure (Fig. 6b and c and Table S2†). To con rm that the change in optical properties is due to the formation of a CdS shell, an XEDS spectrum was collected from a single isolated nanoparticle (Fig. 6d). This clearly demonstrates that Pb, Cd and S are all present in individual particles. Attempts to perform

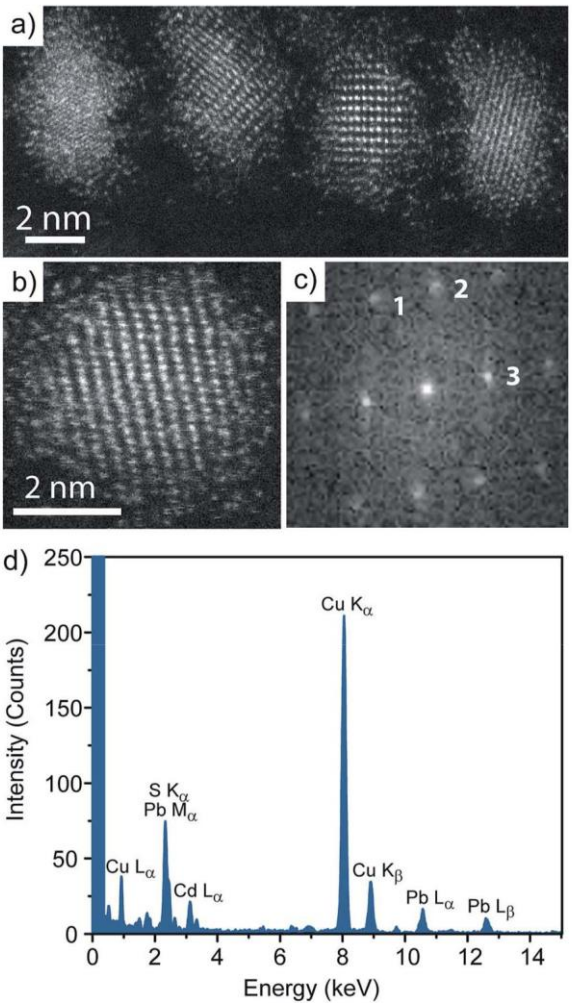

Fig. 6 (a) HAADF-STEM image of several typical biomineralized PbS– CdS core–shell nanoparticles; (b) HAADF-STEM image and (c) corre-sponding fast Fourier transform (FFT) from an individual core–shell morphology particle viewed along the [031] PbS zone axis (detailed fringe fitting is presented in Table S2†); (d) XEDS spectrum collected from a single PbS–CdS nanocrystal, confirming the co-existence of both Pb and Cd cations in the nanocrystal.

XEDS line-scans on individual core–shell particles were unsuccessful, even when utilizing a state-of-the-art JEOL ARM 200CF aberration corrected STEM equipped with a Centurio XEDS silicon dri detector, due to the small size of the particles and their electron beam sensitivity.

There are other possible explanations for the blue-shi noted in the optical properties for the PbS–CdS particles. For instance, a decrease in PbS core particle size by 0.8 nm would generate a blue-shi of 150 nm. However, the consistent size of the PbS seed particles with and without the CdS overlayer as noted from the HAADF-STEM images indicate that this is not the case. Another possibility is the formation of a $Pb_{1-x}Cd_xS$ solid solution via interdiffusion of the two cations within a particle during synthesis. The rapid and progressive blue-shi noted with increasing incubation time (Fig. S1†) indicates that such interdiffusion would have to occur very quickly at the growth temperature, which in our case is only 37 C. We also note from other reports that chemical synthesis of CdS shells on PbS nanoparticles which are typically performed at signi cantly higher temperatures, (i.e. 100 C or higher),[18,19,54,60] can appar-ently generate PbS–CdS core–shell morphology particles without any signi cant cation interdiffusion. Hence we conclude that the blue shi modi cation to optical properties noted in our case arises from the production of PbS–CdS core– shell morphology particles rather than by size erosion of the PbS cores or by $Pb_{1-x}Cd_xS$ alloy formation.

While thicker, typically >2 nm, shells can be directly imaged[57,61] or detected as slight peak shi s in powder XRD patterns,[18] evidence for ultra-thin shells relies on detecting shi s in optical properties analogous to those reported here.[62,63] Thus we cannot with absolute certainty rule out the possibility that CdS shell growth may, in part, occur via the well-known cation exchange reaction.[58,64–67] Pietryga et al. demonstrated that cation exchange between Pb and Cd in the organic phase would result in a 50 nm blue shi at room temperature, which is consistent with our data. This issue is complicated by the presence of the enzyme which we have previously shown to be capable of biomineralizing CdS. We have attempted to remove residual enzyme by utilizing typical enzyme denaturing agents (protease K, SDS, and ethanol), however the addition of these agents leads to quenching of luminescence from the QDs. Evidence for aqueous phase active enzyme-driven CdS shell biomineralization comes from the previously demonstrated CdS biomineralization activity of this class of enzymes in solution and the presence of a small population of pure CdS nanocrystals in the PbS–CdS core–shell solution, as noted in Fig. S3.†

The functionality of our biomineralized PbS and PbS–CdS core–shell quantum dots has been demonstrated in a practical manner by incorporating these nanocrystals into a simple quantum dot sensitized solar cell structure. The current density/voltage (J/V) characteristics of the solar cells containing these two nanoparticle types are compared in Fig. 7. The pure PbS quantum dots yield an open circuit potential, V_{oc}, of 0.43 V, whereas the PbS–CdS core–shell quantum dots improve the V_{oc} to 0.59 V. The V_{oc} values are entirely consistent with previous reports for chemically synthesized PbS–CdS core–shell

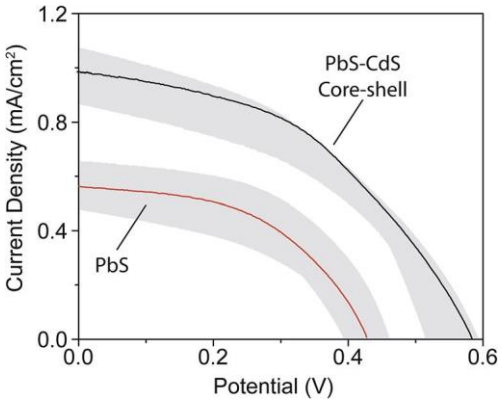

Fig. 7 Current density as a function of cell potential of biomineralized PbS and PbS–CdS core shell quantum dot nanocrystal sensitized solar cells under AM 1.5 illumination. The shaded region represents the reproducibility range achieved between four cells of each type.

quantum dot sensitized solar cells.[26,56,68] The measured increase in V_{oc} is thought to result from passivation of PbS surface defects by growth of the CdS shell.[56] There could also be a slight change due to the blue shi in band-gap of the PbS–CdS core– shell particles.[26] Fill factors for the PbS and PbS–CdS core–shell quantum dot solar cells J–V curves shown were 0.50 and 0.45 respectively. It should be noted that the structure of our solar cell devices has not been optimized and the performance diff erence highlighted here merely serves to (i) illustrate the diff erence between the biomineralized PbS and PbS–CdS core shell nanocrystals and (ii) demonstrate the potential for using these biomineralized quantum dots in real device applications.

Conclusions

We have demonstrated both a biomineralization route to PbS and PbS–CdS core shell quantum con ned nanocrystals and their application in QDSSCs. Biomineralization is facilitated by the extracellular production of a cystathionine g-lyase by an engineered strain of Stenotrophomonas maltophilia with the resulting nanocrystal size controlled through the growth time and temperature. Biomineralized PbS nanocrystals form with the rock-salt structure and demonstrate optoelectronic proper-ties consistent with their size and prior reports of the band gap increase upon PbS quantum con nement. A CdS shell can be biomineralized on the PbS core by addition of cadmium acetate and L-cysteine to the PbS nanocrystals. The resulting quantum dots are amenable to facile phase transfer to an organic phase and lead to enhanced open circuit potential and current density in a QDSSC.

Acknowledgements

This material is based upon work supported by the National Science Foundation under the EFRI-PSBR program, Grant No. 1332349. Additional support was received from the Lehigh University Collaborative Research Opportunity (CORE) program. We thank Robert Dunleavy of the Department of Chemical and Biomolecular Engineering, Lehigh University, for help with sample preparation for electrospray ionization mass spectrometry. We thank Dr Anand Jagota of the Department of Chemical and Biomolecular Engineering, Lehigh University for use of their uorometer.

References

1 S. Mann, Biomineralization: principles and concepts in bioinorganic materials chemistry, Oxford University Press, 2001.

2 F. Nudelman and N. A. Sommerdijk, Angew. Chem., Int. Ed., 2012, 51, 6582–6596.

3 E. M. Pouget, P. H. Bomans, A. Dey, P. M. Frederik, G. de With and N. A. Sommerdijk, J. Am. Chem. Soc., 2010, 132, 11560–11565.

4 C. M. Zaremba, A. M. Belcher, M. Fritz, Y. Li, S. Mann, P. K. Hansma, D. E. Morse, J. S. Speck and G. D. Stucky, Chem. Mater., 1996, 8, 679–690.

5 L. Addadi, S. Raz and S. Weiner, Adv. Mater., 2003, 15, 959–970.

6 K. Shimizu, J. Cha, G. D. Stucky and D. E. Morse, Proc. Natl. Acad. Sci. U. S. A., 1998, 95, 6234–6238.

7 N. Kroger, R. Deutzmann, C. Bergsdorf and M. Sumper, Proc. Natl. Acad. Sci. U. S. A., 2000, 97, 14133–14138.

8 N. Kroger, S. Lorenz, E. Brunner and M. Sumper, Science, 2002, 298, 584–586.

9 D. J. Belton, O. Deschaume and C. C. Perry, FEBS J., 2012, 279, 1710–1720.

10 J. Miot, N. Recham, D. Larcher, F. Guyot, J. Brest and J. Tarascon, Energy Environ. Sci., 2014, 7, 451–460.

11 Z. Yang, L. Lu, V. F. Berard, Q. He, C. J. Kiely, B. W. Berger and S. McIntosh, Green Chem., 2015, 17, 3775–3782.

12 F. W. Wise, Acc. Chem. Res., 2000, 33, 773–780.

13 S. Schmitt-Rink, D. A. B. Miller and D. S. Chemla, Phys. Rev. B: Condens. Matter Mater. Phys., 1987, 35, 8113.

14 R. Vogel, P. Hoyer and H. Weller, J. Phys. Chem., 1994, 98, 3183–3188.

15 R. J. Ellingson, M. C. Beard, J. C. Johnson, P. Yu, O. I. Micic, A. J. Nozik, A. Shabaev and A. L. Efros, Nano Lett., 2005, 5, 865–871.

16 Y. Yang, W. Rodr´ıguez-C´ordoba and T. Lian, Nano Lett., 2012, 12, 4235–4241.

17 W. Shockley and H. J. Queisser, J. Appl. Phys., 1961, 32, 510–519.

18 M. Neo, N. Venkatram, G. Li, W. Chin and W. Ji, J. Phys. Chem. C, 2010, 114, 18037–18044.

19 L. Lai, L. Protesescu, M. V. Kovalenko and M. A. Loi, Phys. Chem. Chem. Phys., 2014, 16, 736–742.

20 Z. Hens, Science, 2015, 348, 1211–1212.

21 S. Seshadri, K. Saranya and M. Kowshik, Biotechnol. Prog., 2011, 27, 1464–1469.

22 M. Kowshik, W. Vogel, J. Urban, S. K. Kulkarni and K. M. Paknikar, Adv. Mater., 2002, 14, 815.

23 H. Bai and Z. Zhang, Mater. Lett., 2009, 63, 764–766.

24 S. Senapati, A. Syed, S. Khan, R. Pasricha, M. I. Khan, R. Kumar and A. Ahmad, Curr. Nanosci., 2014, 10, 588–595.

25 N. Ma, A. F. Marshall and J. Rao, J. Am. Chem. Soc., 2010, 132, 6884–6885.
26 M. Speirs, D. Balazs, H. Fang, L. Lai, L. Protesescu, M. Kovalenko and M. Loi, J. Mater. Chem. A, 2015, 3, 1450–1457.
27 S. Singh, K. Bozhilov, A. Mulchandani, N. Myung and W. Chen, Chem. Commun., 2010, 46, 1473–1475.
28 Y. Kong, F. Gao, R. He, J. Chen, X. Xu, N. Li and D. Cui, Curr. Nanosci., 2010, 6, 446–451.
29 N. Gaponik, D. V. Talapin, A. L. Rogach, A. Eychmuller¨ and H. Weller, Nano Lett., 2002, 2, 803–806.
30 O. E. Semonin, J. C. Johnson, J. M. Luther, A. G. Midgett, A. J. Nozik and M. C. Beard, J. Phys. Chem. Lett., 2010, 1, 2445–2450.
31 P. Kumnorkaew, Y. Ee, N. Tansu and J. F. Gilchrist, Langmuir, 2008, 24, 12150–12157.
32 V. Gonz´alez-Pedro, X. Xu, I. Mora-Sero and J. Bisquert, ACS Nano, 2010, 4, 5783–5790.
33 A. Alonso, P. Sanchez and J. L. Martinez, Antimicrob. Agents Chemother., 2000, 44, 1778–1782.
34 C. Dameron, R. Reese, R. Mehra, A. Kortan, P. Carroll, M. Steigerwald, L. Brus and D. Winge, Nature, 1989, 338, 596–597.
35 G. Chen, B. Yi, G. Zeng, Q. Niu, M. Yan, A. Chen, J. Du, J. Huang and Q. Zhang, Colloids Surf., B, 2014, 117, 199–205.
36 C. Gallardo, J. Monr´as, D. Plaza, B. Collao, L. Saona, V. Dur´an-Toro, F. Venegas, C. Soto, G. Ulloa and C. V´asquez, J. Biotechnol., 2014, 187, 108–115.
37 H. Bai, Z. Zhang, Y. Guo and G. Yang, Colloids Surf., B, 2009, 70, 142–146.
38 D. P. Cunningham and L. L. Lundie Jr, Appl. Environ. Microbiol., 1993, 59, 7–14.
39 M. Koneswaran and R. Narayanaswamy, Sens. Actuators, B, 2009, 139, 104–109.
40 Z. Cai, H. Yang, Y. Zhang and X. Yan, Anal. Chim. Acta, 2006, 559, 234–239.
41 Y. Zhang, H. Zhang, X. Guo and H. Wang, Microchem. J., 2008, 89, 142–147.
42 W. Liu, H. S. Choi, J. P. Zimmer, E. Tanaka, J. V. Frangioni and M. Bawendi, J. Am. Chem. Soc., 2007, 129, 14530–14531.
43 Y. Chen and Z. Rosenzweig, Anal. Chem., 2002, 74, 5132–5138.
44 A. Chatterjee, A. Priyam, S. K. Das and A. Saha, J. Colloid Interface Sci., 2006, 294, 334–342.
45 F. C. van Veggel, Chem. Mater., 2013, 26, 111–122.
46 X. Zhao, J. Yang, L. D. McCormick and J. Fendler, J. Phys. Chem., 1992, 96, 9933–9939.
47 I. Kang and F. W. Wise, J. Opt. Soc. Am. B, 1997, 14, 1632–1646.
48 I. Moreels, K. Lambert, D. Smeets, D. De Muynck, T. Nollet, J. C. Martins, F. Vanhaecke, A. Vantomme, C. Delerue and G. Allan, ACS Nano, 2009, 3, 3023–3030.
49 L. Levina, V. Sukhovatkin, S. Musikhin, S. Cauchi, R. Nisman, D. P. Bazett-Jones and E. H. Sargent, Adv. Mater., 2005, 17, 1854–1857.
50 J. Yang, T. Ling, W. Wu, H. Liu, M. Gao, C. Ling, L. Li and X. Du, Nat. Commun., 2013, 4, 1695.
51 D. Deng, J. Xia, J. Cao, L. Qu, J. Tian, Z. Qian, Y. Gu and Z. Gu, J. Colloid Interface Sci., 2012, 367, 234–240.
52 M. A. Hines and G. D. Scholes, Adv. Mater., 2003, 15, 1844–1849.
53 M. C. Weidman, M. E. Beck, R. S. Hoffman, F. Prins and W. A. Tisdale, ACS Nano, 2014, 8, 6363–6371.
54 Y. Justo, P. Geiregat, K. V. Hoecke, F. Vanhaecke, C. De Mello Donega and Z. Hens, J. Phys. Chem. C, 2013, 117, 20171–20177.
55 I. Moreels, Y. Justo, B. De Geyter, K. Haustraete, J. C. Martins and Z. Hens, ACS Nano, 2011, 5, 2004–2012.
56 G. J. Supran, K. W. Song, G. W. Hwang, R. E. Correa, J. Scherer, E. A. Dauler, Y. Shirasaki, M. G. Bawendi and V. Bulovi´c, Adv. Mater., 2015, 27, 1437–1442.
57 H. Zhao, M. Chaker, N. Wu and D. Ma, J. Mater. Chem., 2011, 21, 8898–8904.
58 H. Zhao, M. Chaker and D. Ma, J. Mater. Chem., 2011, 21, 17483–17491.
59 J. Niu, W. Xu, H. Shen, S. Li, H. Wang and L. S. Li, Bull. Korean Chem. Soc., 2012, 33, 393–397.
60 M. V. Kovalenko, R. D. Schaller, D. Jarzab, M. A. Loi and D. V. Talapin, J. Am. Chem. Soc., 2012, 134, 2457–2460.
61 K. A. Abel, P. A. FitzGerald, T. Wang, T. Z. Regier, M. Raudsepp, S. P. Ringer, G. G. Warr and F. C. van Veggel, J. Phys. Chem. C, 2012, 116, 3968–3978.
62 H. Zhao, H. Liang, F. Vidal, F. Rosei, A. Vomiero and D. Ma, J. Phys. Chem. C, 2014, 118, 20585–20593.
63 J. M. Pietryga, D. J. Werder, D. J. Williams, J. L. Casson, R. D. Schaller, V. I. Klimov and J. A. Hollingsworth, J. Am. Chem. Soc., 2008, 130, 4879–4885.
64 H. Zhou, I. Honma, H. Komiyama and J. W. Haus, J. Phys. Chem., 1993, 97, 895–901.
65 Q. Lin, N. S. Makarov, W. Koh, K. A. Velizhanin, C. M. Cirloganu, H. Luo, V. I. Klimov and J. M. Pietryga, ACS Nano, 2014, 9, 539–547.
66 K. A. Abel, H. Qiao, J. F. Young and F. C. van Veggel, J. Phys. Chem. Lett., 2010, 1, 2334–2338.
67 R. T. Lechner, G. Fritz-Popovski, M. Yarema, W. Heiss, A. Hoell, T. U. Schulli,¨ D. Primetzhofer, M. Eibelhuber and O. Paris, Chem. Mater., 2014, 26, 5914–5922.
68 B. A. Gonfa, H. Zhao, J. Li, J. Qiu, M. Saidani, S. Zhang, R. Izquierdo, N. Wu, M. A. El Khakani and D. Ma, Sol. Energy Mater. Sol. Cells, 2014, 124, 67–74.